Combinational-deformable-mirror adaptive optics system for atmospheric compensation in free space communication

Zhaokun Li [a], Jingtai Cao [a,b], Xiaohui Zhao [a,*], Wei Liu [a]

[a] College of Communication Engineering, Jilin University, 5372 Nanhu Road, Changchun 130012, PR China
[b] Changchun Institute of Optics, Fine Mechanics and Physics, Chinese Academy of Sciences, 3888 Nanhu Road, Changchun 130033, PR China

ABSTRACT

As we know that deformable-mirror (DM) is used in the adaptive optics (AO) systems to compensate atmospheric turbulence in free space optical (FSO) communication system. In order to get rid of the limitations generated by the characters of DM itself, the combinational-deformable-mirror (CDM) adaptive optics (CDM-AO) system is established to correct wave-front aberrations and improve coupling efficiency at the receiver. The analysis of the principle of CDM and the decoupling-working principle based on confinement correction algorithm (CCA) is provided, and the comparison of the correcting results between CDM-AO system and conventional AO system are given. Simulation results indicate that CDM-AO system can correct different aberrations with different characteristics and provide better correction performance than single deformable-mirror (DM) AO system. And the coupling efficiency improvement provided by the correction of AO system is numerically evaluated.

© 2014 Elsevier B.V. All rights reserved.

1. Introduction

FSO is widely concerned among telecommunication community for both space and ground wireless links. It has been mainly considered for last-mile applications [1] due to its large bandwidth potential, unregulated spectrum, relative low power requirement, low BER through coding techniques and ease of redeployment. Since atmospheric turbulence brings phase disturbances along propagation paths that are manifested as intensity fluctuation (scintillation), beam wandering and beam broadening at the receiver, it leads to the significant decrease of coupling efficiency at the receiving terminal [2], which affects the stability and reliability of the FSO communication system [3]. In recent years, some researches have appeared to make efforts to solve this problem [4–7].

Adaptive optics (AO) system is one of the effective methods to improve laser beam quality by the correction of wave-front distortions and has made great achievements [8–13]. Recently, a new method used in AO system to measure and compensate aberrations based on incoherent digital holography is proposed [14–16] which are robust and effective under various ranges of parameters. Some wave-front sensors-less AO systems [17–20] are based on optimization algorithms, such as Genetic Algorithm (GA), Stochastic Parallel Gradient Descent (SPGD), Algorithm of Pattern

Extraction (Alopex) and Simulated Annealing (SA). These algorithms take the information associated with the wave-front aberrations as feedback and control parameters of the correction element and do not use wave-front sensor (WFS) to detect the wave-front aberrations. And this wave-front sensor-less method is low-cost and convenient to implement. Some other papers are devoted to novel means [21,22] related to LOG control or analyze robustness and efficiency of the proposed control strategies in AO systems [23,24].

In the conventional AO systems, a single deformable mirror or other phase correction device are used to compensate for phase distortion. However, the compensation performance of the AO systems largely depends on the characteristics of the deformable mirror (DM), and it is limited by the spatial frequency of the actuators and the stroke [25]. Considering the constraints of the processing speeds, sampling frequency and other technical conditions, the bandwidth of the AO systems only increased to confined extent by the optimized wave-front distortions correction algorithms using the conventional equipments, so creative techniques which get better performance in the bandwidth limitation above depend on the existing equipments are badly needed.

In this paper, the combinational-deformable-mirror (CDM) with two different coupling coefficients is proposed to improve the phase distortions correction capability of AO system and increase the coupling efficiency in FSO communication system. CDM comprises two DMs different from the conventional single DM, and few related researches exist, but some limitations and weaknesses follow. Some researches focus on the increase of the

* Corresponding author. Tel.: +86 139 4488 3530.
E-mail address: xhzhao@jlu.edu.cn (X. Zhao).

spatial resolution by two or more DMs with the same layout and same low spatial resolution [25,26], to compensate the wave-front aberrations, but it requires strict and accurate configuration of the relative spatial location of the actuators belonging to different DMs. Any misstep will degrade the performance of the system and this method is not easy to use in practice. Some researches use two DMs, one with large stroke and another with high spatial frequency, to compensate the aberrations with large scale and high spatial resolution [27]. Some nature of DM itself or the effect of different layout parameters and different coupling coefficients on the compensation is worthy to use and further research about it is necessary. Some researches present a wave-front sensors-less CDM-AO system based on blind optimization by SPGD algorithm [28], but some problems have still existed in current technology with wave-front sensor (WFS).

We focus on analyzing the compensation results due to different layout parameters and different coupling coefficients of DMs themselves theoretically, taking advantage of existing equipments to access the optimal performance of FSO communication system in theory. Theoretical analysis and numerical simulation show that CDM significantly improved the FSO communication system performance. The proposed CDM-AO system can be composed with multiple less-elements DM, which has no strict precision requirement for spatial matching, and the existing control methods or other novel control algorithms can be used in the system based on the existing equipment.

This paper is organized as follows: Section 2 provides the model of FSO communication system and functional block diagram of CDM. Section 3 gives analysis of the advantage of CDM and the double-deformable-mirror decoupling algorithm with the discussion about the coupling efficiency of the FSO receiver. In Section 4, some related simulations are carried out to show the improved correction results of CDM and the performance of FSO communication system. Finally, conclusions are given in Section 5.

2. System model

The functional block diagram of FSO communication system and the configuration of the spatial combination of the two DMs are shown in Fig. 1(a) [2] and Fig. 1(b).

Atmospheric disturbances reduce the fiber coupling efficiency at the receiving terminal and seriously affect communication performance. In order to overcome this problem, AO system with a wave-front sensor, a wave-front corrector and a wave-front controller can correct phase distortions brought by the disturbances. Generally, Shack Hartmann wave-front sensor (S–H sensor) is used to measure the optical phase deviations of the incoming wave-front. Then the wave-front controller computes suitable DM deformations to compensate wave-front aberrations when the transmitted laser is reflected from the wave-front corrector (a deformed DM). Finally, DM receives the deformation commands as fast as possible to achieve desired optical correction [26]. The laser signal through the atmospheric turbulence is divided into two beams [2], one is used for wave-front measurement and other is coupled into a single mode fiber and received by the optical receiver.

To ensure the robust stability of pupils, the conjugate relation between the wave-front in the CDM-AO system is important. Appropriately change the aperture of laser beam to fit the size of each DM, we use lenses and mirrors to compose the conjugate wave-front phase optical systems which are necessary for the sizes of DMs are fairly different. Generally speaking, the DMs can access KHz bandwidth and the above frequencies. And adaptive optics systems operate at high frequencies, typically several hundred to several thousand Hz [29]. Since wave-front corrector is an inertia

link and cannot response for a sudden transition input signal, CDM-AO system will slightly decrease in bandwidth but also in the above frequency range.

3. Analysis of combinational deformable mirror

3.1. Model and parameters of DM

Approximate the DM's influence function by the Gaussian Model

$$S_j(x,y) = \exp\left\{\ln \omega \left[\frac{1}{d}\sqrt{(x-x_j)^2 + (y-y_j)^2}\right]^\alpha\right\} \quad (1)$$

where ω is the coupling coefficient, determined by the sizes of electrode actuators and the DM. $\left(x_j, y_j\right)$ is the center coordinate of the jth actuator. d is the normalized interval between the adjacent actuators, and α at the index position is the Gaussian index. The phase compensation $u(x,y)$ generated by the deformable mirror is given by

$$u(x,y) = \sum_{j=1}^{N} v_j S_j(x,y) \quad (2)$$

where v_j is the jth voltage of the actuators, N is the number of actuators. We can obtain that the numeral relationship between the phase aberration generated by the DM and voltages applied on the actuators is linear.

In this paper, two groups of DM are chosen and they are very different in coupling coefficient and size. In general, DM with high coupling coefficient and low spatial solution in normal circle obtains better compensation for large-scale low-order aberrations while DM with low coupling coefficient and high spatial solution in normal circle offers better compensation for small-scale high-order aberrations.

The actuators mainly have three configuration modes: circular arrangement, square arrangement and triangle arrangement. The configurations of subapertures of S–H sensor and deformable mirror actuators in Group 1 are shown in Fig. 2. Fig. 2(a) describes a 19-element DM, and a 61-element DM is illustrated in Fig. 2(b), in which both groups meet triangle arrangement. In Group 2, the 32-element DMs with square arrangement mode (Fig. 2(c)) and the 61-element DM in Fig. 2(b) are used. In Fig. 1, we know that the coupling efficiency of DM1 is higher so DM1 could be tiny, but DM2 is on the contrary. DMs are mainly not with same coupling coefficient and size. DM1 compensates for large-scale low-order aberrations, and DM2 compensates for small-scale high-order aberrations.

3.2. Decouple the aberration by CCA

Take DM2 in Group 1 as an example to analyze the decoupling subject. In theoretical analysis, we take samples of the normalized wave-front aberrations generated by DM2 in unit circle (the step length is 0.005).DM2 is used to compensate for small-scale high-order aberrations. The introduced high-order aberrations are sampled and expressed by a vector. Ideally, DM2 can generate wave-front aberrations as same as the high-order aberrations, while the effect on low-order aberrations should be as little as possible, which can be written as

$$\mathbf{W}_H = \mathbf{R}_{2H}\mathbf{v_2} \quad (3)$$

$$0 = \mathbf{R}_{2L}\mathbf{v_2} \quad (4)$$

where $\mathbf{W}_H$ is a vector that its elements are the sampled values of the introduced high-order aberration, $\mathbf{R}_{2H}$ is a matrix, its element $\mathbf{R}_{i,j}$ presents the impact factor of the jth actuator's voltage on the ith sampled value of the high order phase aberration. $\mathbf{R}_{2L}$ is similar, each element can be obtained by Eq. (1). Due to the orthogonality
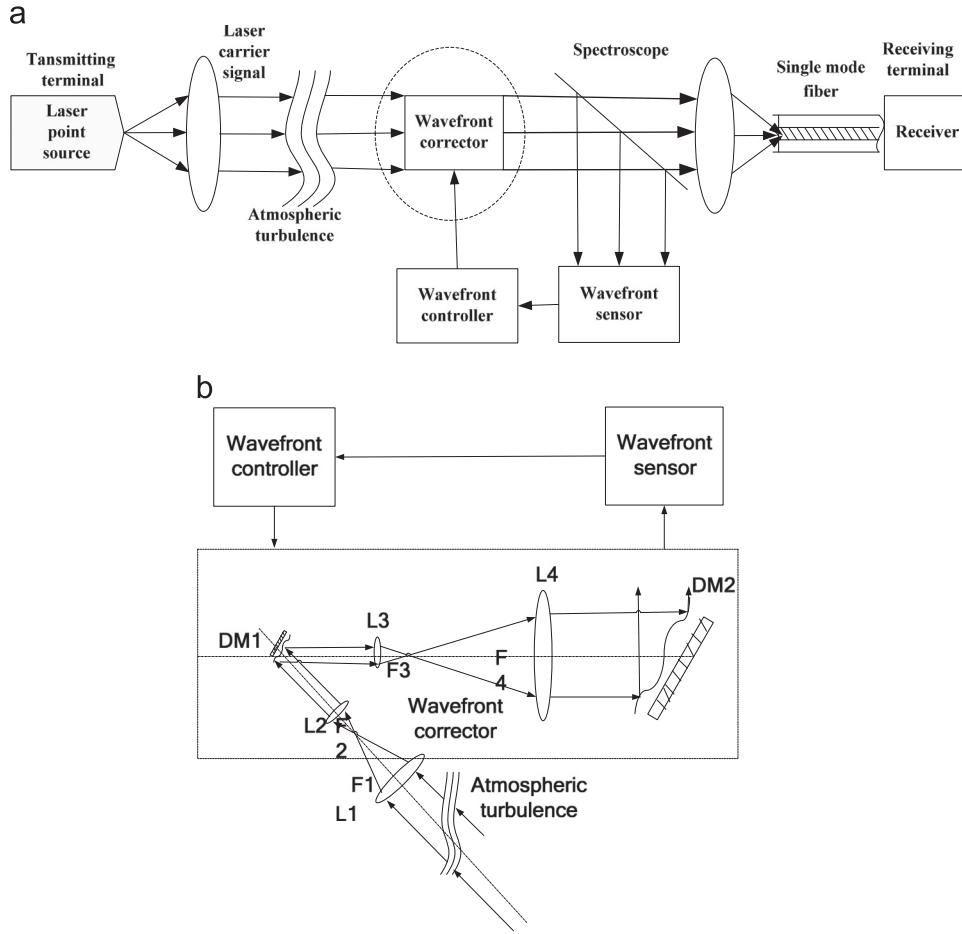
Fig. 1. Functional block diagram of the system. (a) Functional block diagram of FSO system and (b) Conjugate wave-front system of CDM.

of Zernike polynomial [30], we can obtain that

$$\iint_S Z_L Z_H dxdy = 0 \tag{5}$$

where S is the normalized unit circle, Z_H and Z_L represent the high-order and low-order aberration respectively, and can be written as

$$Z_L = \sum_{i=1}^{l} a_i Z_i \tag{6}$$

$$Z_H = \sum_{i=l+1}^{\infty} a_i Z_i \tag{7}$$

When using DM to fit the high-order aberration, we have

$$Z_H = \sum_{m=1}^{61} v_m S_m(x,y) \tag{8}$$

where v_m is the voltage of the mth actuators. From Eq. (5) to Eq. (8), we obtain

$$\sum_{m=1}^{61} v_m \iint_S Z_L S_m(x,y)dxdy = 0 \tag{9}$$

let $r_{mL} = \iint_S Z_L S_m(x,y)dxdy$, thus

$$\sum_{m=1}^{61} v_m r_{mL} = 0 \tag{10}$$

So Eq.(5) can be written as

$$0 = (r_{1L},\ r_{2L},\ \ldots,\ r_{61L})\mathbf{v_2} \tag{11}$$

By solving the following linear equation

$$\begin{pmatrix} \mathbf{W}_H \\ 0 \end{pmatrix} = \begin{pmatrix} \mathbf{R}_{2H} \\ r_{1L},\ \cdots,\ r_{61L} \end{pmatrix} \mathbf{v}_2 \tag{12}$$

The least square solution

$$\mathbf{v}_2 = \begin{pmatrix} \mathbf{R}_{2H} \\ r_{1L},\ \cdots,\ r_{61L} \end{pmatrix}^+ \begin{pmatrix} \mathbf{W}_H \\ 0 \end{pmatrix} \tag{13}$$

is the voltage vector applied to the actuators, where $\begin{pmatrix} \mathbf{R}_{2H} \\ r_{1L},\ \cdots,\ r_{61L} \end{pmatrix}^+$ presents the pseudo-inverse of matrix $\begin{pmatrix} \mathbf{R}_{2H} \\ r_{1L},\ \cdots,\ r_{61L} \end{pmatrix}$. The analysis of DM1 is similar. It allows CDM to function at peak according to its own characteristics and the distribution characteristics of phase aberrations.

3.3. Analysis of the performance of FSO communication system

In both natural light and laser FSO communication systems, far-field intensity distribution is determined by diffraction limit and the wave-front aberrations from atmospheric turbulence. The wave-front aberrations both systems are approximated by Zernike polynomial. In the receiver, the appearance of the errors is mainly the optical energy loss in the free space propagation path. The following analysis is suitable for both natural light and laser FSO communication systems.

The goal of a conventional adaptive optics system is to minimize the residual phase aberrations after the incoming wave
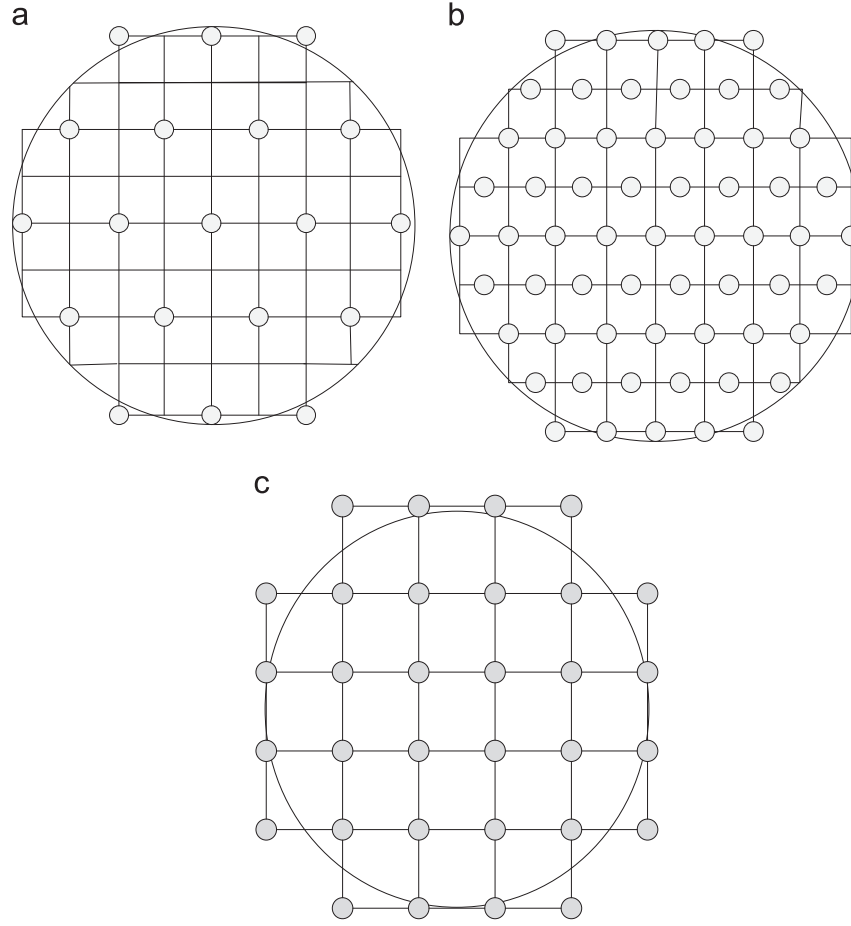
Fig. 2. Configurations of subapertures (squares) and deformable mirror actuators (filled circles). (a)19-element, (b) 61-element and (c) 32-element.

passes the deformable mirror. This corresponds to the maximization of the Strehl Ratio (ST), which is defined as the ratio of the actual maximum intensity of the zero order diffraction spot and its theoretical upper limitation for an undistorted wave.

Generally, the received laser signals are coupled into a single mode fiber, so the coupling efficiency of single mode fiber, defined as the ratio of the average power coupled into the fiber to the average power in the receiver aperture plane [31], has significant influence on the performance of FSO system. Ideally, spatial light beam converges to a point after passing through the optical system, and generates Airy disk on the focal plane. Its optical distribution has relationship in Fourier transform with the entrance pupil. The single-mode fiber on the focus plane is used to couple the light. The basic theory of coupling is the mode matching between the Airy disk and the single-mode fiber, and higher matched degree means higher coupling efficiency. The lateral and axial offset is neglected in order to provide an emphasis on the problem. For the estimation of the coupling efficiency, we only deal with single-mode fiber coupling, and the fiber diameter is 10 μm. The coupling efficiency can be expressed as

$$J \propto \frac{\left| \iint A_f(r) M_0^*(r) d^2 r \right|^2}{\iint A_f(r) A_f{}^*(r) d^2 r \times \iint M_0(r) M_0^*(r) d^2 r} \tag{14}$$

where $A_f(r)$ is the Fourier transform of single-mode fiber optical field, $M_0(r)$ is the incident optical field in the focal plane, $A_f(r)$ and $M_0(r)$ are complex quantities. Since Eq. (12) is too complex to calculate, we apply ST to simplify the average coupling efficiency

[31,32] given by

$$ST \propto \left| A_f(r_0) \right|^2 \tag{15}$$

where r_0 is the desired on-axis location of the center of the fiber. Assume that the wave-front phase aberration satisfies Gauss distribution, then ST can be estimated by variance RMS^2 as follow

$$ST \propto \exp(-\text{RMS}^2) \tag{16}$$

When RMS^2 is close to zero, we can get a easier formula

$$ST \propto 1 - \text{RMS}^2 \tag{17}$$

In practice, pixel size of CCD camera approximately equals to the fiber diameter, ST is expressed as [2]

$$ST = \frac{|\max[A(i)]|^2}{|\sum_{i=1}^{N}[A(i)]^2|} \tag{18}$$

where $A(i)$ is the gray value of the ith pixel, and N is the number of pixels. The basic parameters of CCD are shown in Table 1.

4. Numerical simulations

In numerical simulations, we introduce some groups of original wave-front aberrations under strong turbulence, thus atmospheric coherent length is very small (about 5–6 cm) [33]. Assume that the limitation of stroke is enough and the receiving aperture is 120 cm, so that we focus on the correction results related to the layout mode and the coupling coefficient of DMs. We also assume that the wave-front aberration satisfies Gauss distribution, without considering

the noise and the energy loss of AO system, the analysis of the coupling efficiency is provided.

We use the first 25 order Zernike polynomial (regardless of the phase slopes) to fit the introduced wave-front aberrations. Define

the fitting error as:

$$E_{FE} = \frac{RMS_R}{RMS_C} \qquad (19)$$
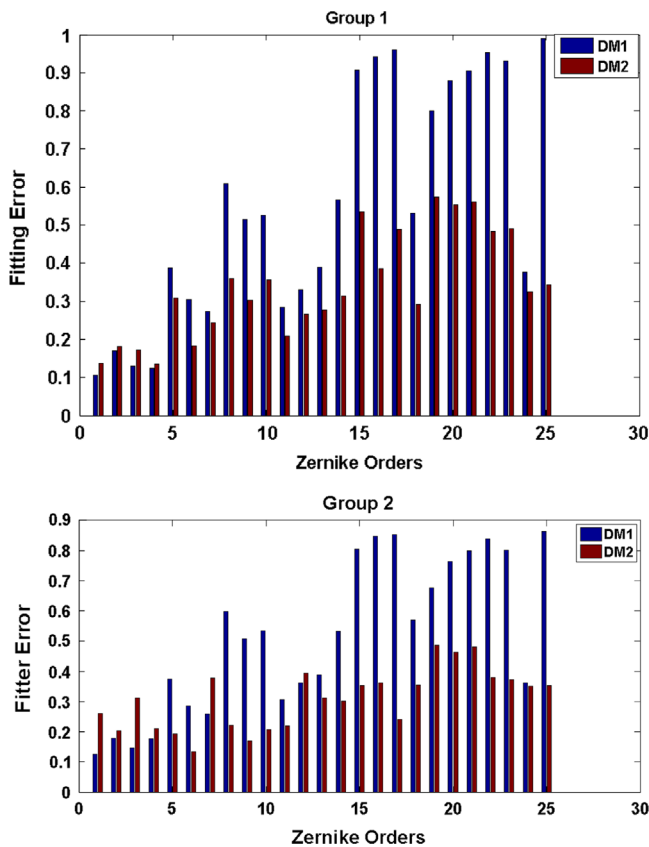
Eq. (19) presents fitting capability for wave-front aberrations of DM. Where RMS_C presents RMS value of the wave-front phase aberration before correction and RMS_R presents RMS value of the residual wave-front phase aberration after correction. The smaller E_{FE} is, the more precise wave-front aberrations DM generates. The fitting capabilities of two DMs for each Zernike order are shown in Fig. 3 (Group 1 and Group 2). Although with the increasing corrected orders, the performance will be improved, but too many high orders will lead to amount of calculation and finite improvement, so the lower-orders correcting can get a satisfied performance. Apparently, DM1 with higher coupling efficiency has better performance on correcting low-order (1–4 order in Group1, 1- order in Group2) phase aberrations, the DM2, in fact, the contrary is the case.

The Zernike coefficients of 5 groups of introduced wave-front aberrations are shown in Table 2. Numerical simulations about the wave-front aberrations correcting with CDM (take Group 1 for example) and comparisons with a single DM (19- or 61- element DM) are performed and shown in Table 3.

It is obvious that the correcting result of CDM has significant improvement compared with the 19-element DM and the 61-element DM in each group.

For the optimization algorithms used in AO systems such as SPGD Algorithm [8,34] and SA Algorithm [35] without S–H sensor (sensor-less), it doesn't seems that CDM will improve the rate of convergence or the final metric (ST or RMS) of AO systems because these algorithms have no requirement for the wave-front aberrations fitting capability of DMs. The Wave-front aberrations correction using SPGD is shown in Fig. 4.
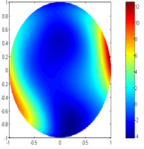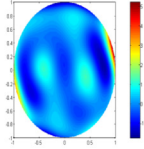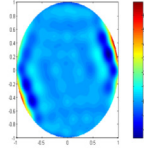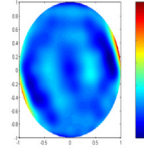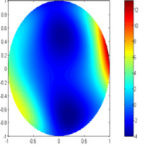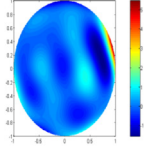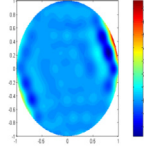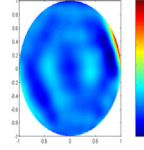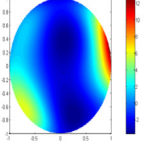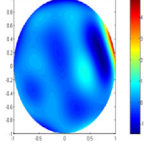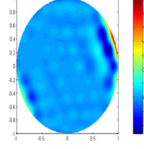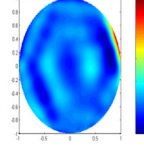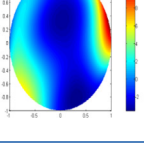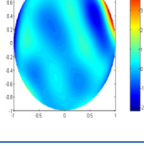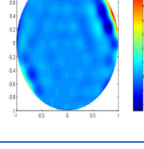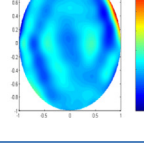
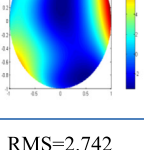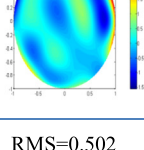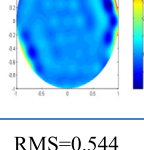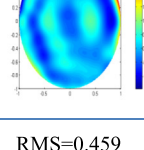Fig. 5 shows the approximate relationship between the average coupling efficiency and the RMS of wave-front aberrations, according to Eq. (15) and Eq. (16).

Due to the reduced RMS of residual wave-front aberrations by CDM, the coupling efficiency at the FSO receiver is improved, the performance of FSO communication system is significantly improved. Here we do not consider the power loss generated by single mode fiber and the detailed data is shown in Table 4 (Group 1). We can get the coupling efficiency by Eq. (16) or Eq. (17), in order to get the accurate theoretical value, Eq. (16) is recommended.

Table 1
Basic parameters of CCD.

Pixel size	$9.9\ \mu m \times 9.9\ \mu m$
Resolution	256×256
Frame rate	1076

Fig. 3. Fitting capability of DM1 and DM2 for each Zernike order.

Table 2
Zernike coefficients of 5 groups of introduced wave-front aberrations.

No.	4th Order	5th Order	6th Order	7th Order	8th Order	9th Order	10th Order	11th Order	12th Order
1	3.50	3.00	2.30	1.25	−0.32	0.30	−0.28	0.28	0.30
2	3.50	3.00	2.15	1.30	0.52	0.30	0.29	0.28	−0.30
3	3.10	2.95	2.15	1.80	0.82	0.30	0.29	−0.28	−0.30
4	2.90	2.65	2.15	1.76	0.82	0.70	0.39	−0.28	−0.27
5	2.87	2.63	1.97	1.56	0.81	0.73	0.39	−0.32	−0.29

No.	13th Order	14th Order	15th Order	16th Order	17th Order	18th Order	19th Order	20th Order	21th Order
1	0.29	−0.27	0.28	0.26	−0.26	0.25	−0.25	0.24	0.25
2	−0.30	−0.26	0.25	0.26	−0.25	0.25	−0.22	0.24	0.25
3	0.27	−0.26	0.25	0.25	−0.24	0.23	−0.22	0.21	0.20
4	0.27	−0.26	0.25	0.24	−0.24	0.23	−0.22	0.20	0.20
5	0.27	−0.26	0.26	0.25	−0.24	0.23	−0.21	−0.20	−0.19

No.	22th Order	23th Order	24th Order	25th Order	26th Order	27th Order	28th Order
1	−0.26	0.24	−0.23	0.23	0.22	0.21	0.19
2	−0.26	0.20	−0.19	0.19	0.18	0.17	0.15
3	−0.18	0.17	−0.16	0.14	0.14	0.12	0.10
4	−0.18	−0.17	0.15	−0.14	0.13	0.12	0.10
5	0.18	−0.16	0.15	0.14	−0.13	0.12	−0.09

Table 3
Comparison of wave-front aberrations correcting between CDM and a single DM.

NO.	Introduced wave-front aberrations	Residual wave-front aberrations with only DM1	Residual wave-front aberrations with only DM2	Residual wave-front aberrations with CDM
1				
	RMS=3.064	RMS=0.689	RMS=0.721	RMS=0.563
2				
	RMS=3.038	RMS=0.618	RMS=0.656	RMS=0.530
3				
	RMS=2.976	RMS=0.551	RMS=0.586	RMS=0.496
4				
	RMS=2.835	RMS=0.578	RMS=0.578	RMS=0.512
5				
	RMS=2.742	RMS=0.502	RMS=0.544	RMS=0.459

5. Conclusions

In this paper, CDM-AO system is proposed, which uses combinational-deformable-mirror (CDM) instead single DM. CDM comprised of two DMs, one's coupling coefficient is large and another is small, are required to cooperate to compensate for the aberrations. DM1 compensates for large-scale low-order aberrations, and DM2 compensates for small-scale high-order aberrations. CDM-AO system can correct the wave-front aberrations whose spatial frequency is higher than the single DM can correct. The numerical simulation has validated that CDM can enhance the spatial frequency and wave-front correction capability of phase compensation. Thus, CDM-AO system can improve wave-front correction capability without increasing cost of manufacture and control. This scheme can be used easily in the FSO communication system.

The performance of FSO communication system is analyzed, the result shows that the average coupling coefficient increases and the dissipation of energy is reduced. Therefore, the FSO communication system performance is improved obviously. It makes perfect sense in some cases, e.g. phase aberrations with high spatial resolution or strict performance requirements for FSO communication system.
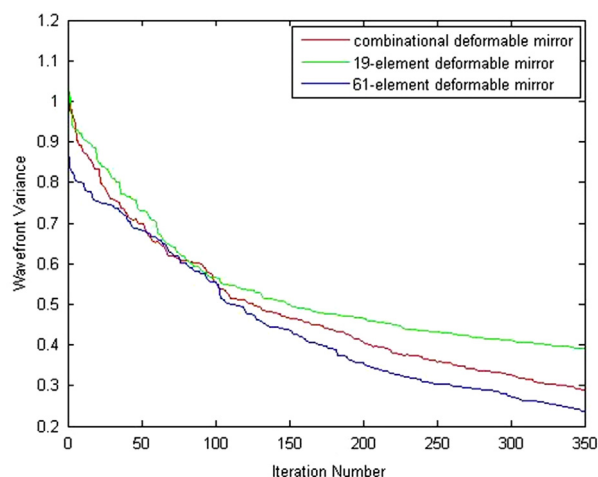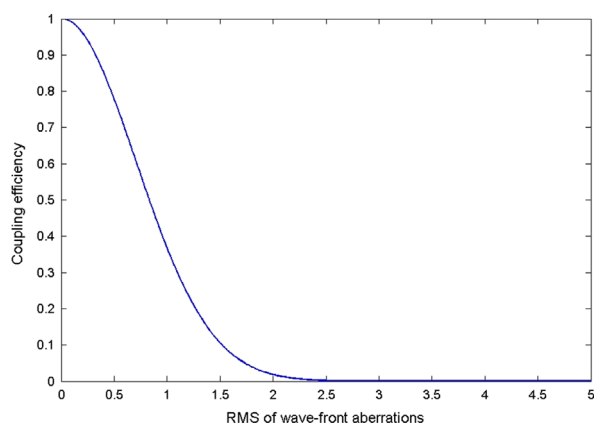
Fig. 4. Phase aberration correction by SPGD.

Fig. 5. Relationship between average coupling efficiency and RMS of wave-front aberrations.

Table 4

Comparison of coupling efficiency at the FSO receiver between CDM- and single DM-AO system.

No.	Initial coupling efficiency (%)	Coupling efficiency with only DM1 (%)	Coupling efficiency with only DM2 (%)	Coupling efficiency with CDM (%)
1	0.0084	62.24	59.47	72.80
2	0.0098	68.22	64.99	75.52
3	0.0142	73.83	71.08	78.22
4	0.0323	71.62	71.68	76.94
5	0.0543	77.69	74.42	80.97

Acknowledgement

References

[1] Mohammad Abtahi, IEEE 24 (12) (2007) 4966.
[2] Wei Liu, Wenxiao Shi, Opt. Commun. 309 (2013) 212.
[3] Song Dongyiel, Hurth Yoon Such, Cho Jin Woo, Opt. Express 7 (2000) 280.
[4] Hans Bruesselbach, L. Minden Monica, Wang Shuoqin, SPIE 5338 (2004) 90.
[5] Wei Liu, Wenxiao Shi, Jingtai Cao, Optik (2013).
[6] Huizhen Yang, Xinyang Li, IEEE (2009) 338.
[7] Yuhui Chen, Lu Huang, Lin Gan, Zhiyuan Li, Light: Sci. Appl. (2012).
[8] Mikhail A. Vorontsov, J. Opt. Soc. Am. A 19 (2) (2002) 356.
[9] Enrico Fedrigo, Riccardo Muradore, Davide Zilio, Control Eng. Pract. 17 (1) (2009) 122.
[10] Jens Schwarz, Marc Ramsey, Opt. Commun. 264 (1) (2006) 203.
[11] Chao Liu, Lifa Hu, Opt. Commun. 285 (3) (2012) 238.
[12] Lisa Poyneer, Jean-Pierre Véran, J. Opt. Soc. Am. A 25 (7) (2008) 1486.
[13] Douglas P. Looze, Eur. J. Control 3 (2011) 237.
[14] Myung K. Kim, Opt. Lett. 37 (13) (2012) 2694.
[15] Myung K. Kim, Appl. Opt. 52 (1) (2013) A117.
[16] Changgeng Liu, Xiao Yu, Myung K. Kim, Appl. Opt. 52 (12) (2013) 2940.
[17] Ping Yang, Yuan Liu, Opt. Lasers Eng. 46 (7) (2008) 517.
[18] Huizhen Yang, Xinyang Li, Opt. Laser Technol. 43 (2011) 630.
[19] H. Song, R. Fraanje, Opt. Express 18 (23) (2010) 24070.
[20] Jacopo Antonello, Michel Verhaegen, J. Opt. Soc. Am. A 29 (11) (2012) 2428.
[21] Caroline Kulcsár, Henri-François Raynaud, Automatica 48 (2012) 1939.
[22] Carlos Correia, Henri-François Raynaud, Eur. J. Control 3 (2011) 222.
[23] Lucie Baudouin, Christophe Prieur, Appl. Opt. 47 (20) (2008) 3637.
[24] Andres Guesalaga, Benoit Neichel, Opt. Express 21 (9) (2013) 10676.
[25] Huafeng Yang, Guilin Liu, Chin. Opt. Lett. 5 (8) (2007) 435.
[26] Liu Guilin, Yang Huafeng, Chin. Opt. Lett. 5 (10) (2007) 559.
[27] Shijie Hu, Bing Xu, Appl. Opt. 45 (12) (2006) 2638.
[28] Xiang Lei, Shuai Wang, Opt. Express 20 (20) (2012) 22143.
[29] J.K. Gruetzner, S.D. Tucker, SPIE 2534 (1995) 94.
[30] Guangming Dai, J. Opt. Soc. Am. A 12 (10) (1995) 2182.
[31] Yasser M. Sabry, Bassam Saadany, Diaa Khalil, Light: Sci. Appl. (2013).
[32] Thomas Weyrauch, Mikhail A. Vorontsov, SPIE 4489 (2002) 177.
[33] R.J. Noll, J. Opt. Soc. Am. 66 (3) (1976) 207.
[34] Mikhail A. Vorontsov, Gary W. Carhart, J. Opt. Soc. Am. A 17 (8) (2000) 1440.
[35] Yuping Zhang, Zhaori Deng, Ruiqi Zhang, IEEE (2013) 209.